electronics

Review

Advances and Perspectives in Multilevel Converters: A Comprehensive Review

Alessandro Benevieri, Simone Cosso, Andrea Formentini, Mario Marchesoni, Massimiliano Passalacqua and Luis Vaccaro *

Department of Electrical, Electronic, Tlc Engineering and Naval Architecture (DITEN), University of Genova, Via all'Opera Pia 11a, 16145 Genova, Italy; alessandro.benevieri@edu.unige.it (A.B.); simone.cosso@edu.unige.it (S.C.); andrea.formentini@unige.it (A.F.); marchesoni@unige.it (M.M.); massimiliano.passalacqua@unige.it (M.P.)
* Correspondence: luis.vaccaro@unige.it

Abstract: In contemporary power electronics, multilevel converters stand at the forefront of high-power, high-voltage applications, offering superior performance in terms of efficiency, reduced harmonics, and improved voltage waveform quality compared to traditional two-level converters. Their capability to synthesize waveforms with multiple voltage levels has garnered significant attention across various industrial sectors, including renewable energy systems, electric vehicles, and high-voltage power transmissions. This paper provides a comprehensive overview of multilevel converter technology, encompassing their classification, main topologies, recent advancements, and emerging trends. By exploring the evolution of multilevel converter technology and identifying future research directions, researchers and engineers can gain valuable insights into the design, optimization, and application of these advanced power electronic systems.

Keywords: voltage source inverter (VSI); power electronics; multilevel converters (MLCs); medium-voltage drives; power converters; high-power applications; topologies; modulation

check for updates

Citation: Benevieri, A.; Cosso, S.; Formentini, A.; Marchesoni, M.; Passalacqua, M.; Vaccaro, L. Advances and Perspectives in Multilevel Converters: A Comprehensive Review. *Electronics* **2024**, *13*, 4736. https://doi.org/10.3390/electronics13234736

Academic Editors: Ahmed Abu-Siada and Jingyang Fang

Received: 14 October 2024
Revised: 2 November 2024
Accepted: 21 November 2024
Published: 29 November 2024

1. Introduction

Multilevel converters (MLCs) play a pivotal role in modern industry applications [1–3]. In recent years, they have been widely used in various medium-voltage, high-power applications, in particular in a continuous renewable energy extension scenario [4–6]. Since their initial introduction in the industry and academic literature, MLCs have become a focal point of study, research, and innovation among engineers and researchers [7–9]. Among all the different fields where MLCs have found widespread employment in recent decades, high-voltage direct-current (HVDC) power systems, static compensators (STATCOM), flexible AC transmission systems (FACTS), and large motor drives are mentioned [10–13].

MLCs operate on the principle of producing a staircase waveform voltage employing power semiconductor devices. Additionally, capacitors, batteries, and renewable energy resources can serve as DC links [14–16]. By synthesizing high-voltage outputs through various combinations of input voltage levels, MLCs enable switches to have low-voltage ratings, which are closely aligned with the voltage levels of the input DC sources.

As a direct consequence, MLCs offer superior performance compared to conventional two-level converters, exhibiting advantages such as a modular structure, a better harmonic content, a reduced voltage stress (dv/dt) [17], and a reduced electromagnetic interference [17–19], lower switching losses due to reduced switching frequency, fault-tolerant operation capability [20], and a reduced common-mode output voltage [21].

The great advancements and improvements in power converters of recent years has been propelled by the emergence of high-performance microprocessors capable of executing advanced nonlinear digital-control algorithms. Additionally, significant progress in power electronic semiconductor technology has led to the development of new high-speed switching devices with remarkably low on-state losses. Among these promising power electronic semiconductors, silicon carbide (SiC) and gallium nitride (GaN) devices stand out for their dynamic behavior, particularly in high-switching-frequency applications [20–22]. Consequently, these advancements enabled the design of more compact power electronic converters compared to traditional counterparts. Recent advancements in multilevel converter technology have been significant, driven by the growing need for high-power, high-efficiency conversion systems across various industrial applications, including renewable energy integration, electric vehicles, and grid-connected systems. The introduction of new semiconductor devices, coupled with innovative control algorithms and modulation schemes, has further enhanced the capabilities and performance of multilevel converters.

Despite this progress, several challenges and opportunities remain for future research and development in the field of multilevel converters. The key areas of focus include optimizing converter topologies for specific applications, improving efficiency and reliability, integrating advanced control and modulation techniques, and exploring new semiconductor materials and device technologies. Additionally, thermal management remains a critical concern, particularly in high-power applications. Ongoing research is dedicated to addressing these challenges, emphasizing advanced control strategies and the incorporation of intelligent fault-detection mechanisms.

This paper aims to describe the multilevel converter topologies that have gained more relevance in recent years, and it will be structured as follows: Sections 2 and 3 will be focused on the description of the three classical multilevel architectures, and the main modulation techniques. The recent advances in terms of new topologies are contained in Section 4, while future trends and perspectives are contained in Section 5 and conclusions are drawn in Section 6.

2. Classical Multilevel Structures

The development of multilevel converters commenced with the concept of the multilevel stepped waveform concept, utilizing a series-connected H-bridge, commonly referred to as the cascaded H-bridge converter, in the late 1960s [23]. Concurrently, advancements in low-power applications led to the introduction of a flying capacitor (FC) topology in the same period [24]. Subsequent progress in the late 1970s saw the introduction of the diode-clamped converter (DCC) [25]. The DCC concept evolved further into the three-level neutral-point-clamped (3L-NPC) converter, which we recognize today as the first practical multilevel power converter for medium-voltage applications [26]. Additionally, the cascaded H-bridge (CHB) topology resurfaced in the late 1980s [27], gaining more industrial significance in the mid-1990s. Similarly, the early FC circuit concept, initially designed for low power in the 1960s, transformed into the medium-voltage multilevel converter topology we are familiar with today during the early 1990s [28].

The three multilevel converter topologies discussed herein are now regarded as the classical or traditional options, having transitioned into real industrial products over the past two decades. Figures 1–3 illustrate the architecture of a single-phase circuit for each of these topologies. These topologies are readily accessible from diverse producers, presenting a variety of power ratings, front-end setups, cooling mechanisms, semiconductor selections, and control methodologies, alongside other technical specifications.

Among these different multilevel topologies, the NPC and the CHB have emerged as the most favored options in the industry, each with its own distinct characteristics. The CHB excels in achieving higher voltage and power levels. In contrast, the NPC features a simpler circuit structure, leading to a smaller physical footprint. When it comes to the types of devices used, the NPC typically employs medium- to high-voltage components, such as integrated gate-commutated thyristors (IGCTs) and medium-/high-voltage insulated-gate bipolar transistors (IGBTs), whereas the CHB can utilize low-voltage IGBTs. Furthermore, the NPC configuration is particularly well suited for back-to-back regenerative applications, while the CHB topology requires a greater number of devices to achieve regenerative operation, needing a three-phase two-level VSI for each cell. Despite both configurations generating the same number of levels with an equal number of switching devices, the CHB offers a wider range of output voltage levels (up to 15) resulting in a lower average switching frequency for the devices. The following section will provide a detailed description of these three classical multilevel topologies.

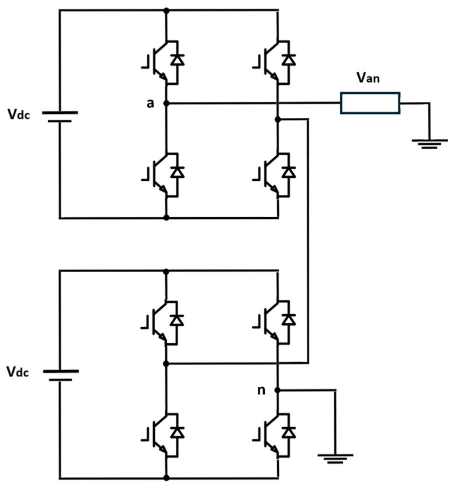

Figure 1. One phase of a CHB architecture.

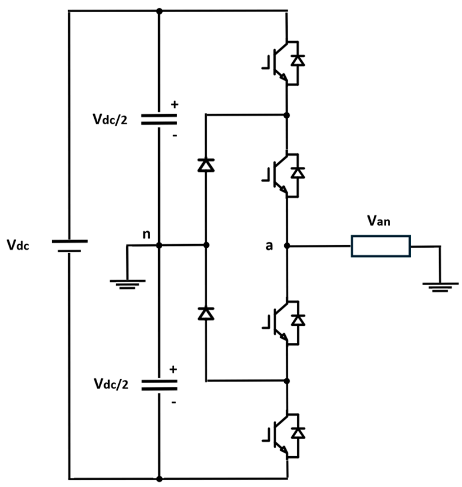

Figure 2. One phase of a NPC architecture.

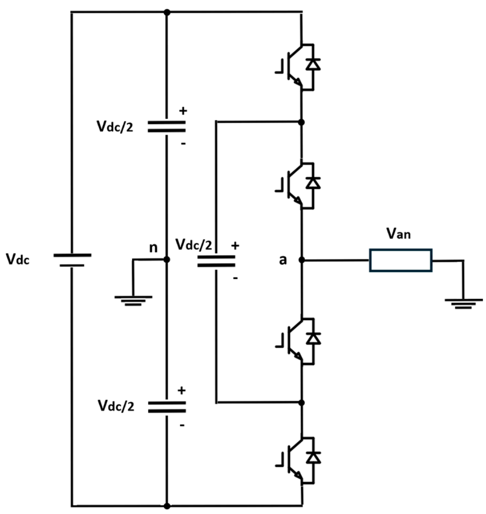

Figure 3. One phase of a FC architecture.

3. Classical Multilevel Topologies Description

3.1. Neutral Point Clamped

This topology, since it has been introduced in the early 1980s [26], proposed as an extension of the existing two-level voltage-source converter (2L-VSC), aimed to overcome limitations in voltage and power ranges imposed by the blocking voltages of semiconductor devices with active turn-on and turn-off capabilities. By ensuring all semiconductors operated at a switching voltage of half the DC-link voltage, the 3L-NPC provided a straightforward solution, particularly beneficial for medium-voltage (MV) applications ranging from 2 to 5 kV [29,30]. The topology gained rapid traction in the market after its introduction by leading manufacturers and became increasingly significant. Essentially, the three-level power circuit of the 3L-NPC-VSC incorporates extra diodes per phase leg compared to the 2L-VSC. This design allows for the connection of the phase output to the neutral point n of the converter, thus enabling the distinctive three-level operation. While various extensions of NPC converters have been proposed to generate additional output voltage levels [31], some of these have yet to gain industrial acceptance [31–34].

The overall switching state of the converter is defined by the combination of switching states across all three phases, with each phase's switching state represented as either generating Vdc/2, −Vdc/2, or being connected to the neutral point (generating a zero-voltage level). The 3L-NPC-VSC encompasses 27 switch states, calculated as L^3, where L represents the number of voltage levels of each phase v_{xN} (x = a, b, c). These switch states can be visualized in the complex $\alpha-\beta$ frame by computing the associated space vector for each switching state, with certain states exhibiting redundant space vector representations, which can be utilized for neutral-point balance purposes [35–37].

$$\begin{aligned} v_s &= \tfrac{2}{3}\left[v_{aN} + a v_{bN} + a^2 v_{cN}\right] \\ &= \tfrac{2}{3}\left[S_a \tfrac{V_{dc}}{2} + a S_b \tfrac{V_{dc}}{2} + a^2 S_c \tfrac{V_{dc}}{2}\right] \end{aligned} \quad (1)$$

Table 1 shows the switching states for a single phase of a 3L-NPC.

Table 1. Single phase 3L-NPC switching table.

Output Voltage VaN	Gate Signals Sa1	Sa2	Switching State Sa
Vdc/2	1	1	+
0	0	1	0
−Vdc/2	0	0	−

3.2. Cascaded H-Bridge

The cascaded H-bridge (CHB) was first introduced in 1988 [27], and it rapidly became one of the most interesting solutions in the following years. It operates through the series connection of H-bridge power cells, earning it the designation of a multicell inverter [38–40]. Each cell comprises a single-phase HB converter, a capacitive DC link, a rectifier, and an autonomous voltage source, such as batteries or transformer secondaries [41–43]. The rectifying stage can be a full bridge where diodes are used, whereas an active front end (AFE) is needed when regenerative operation is required [44–47].

Considering the inverter side of the power cells depicted in Figure 4, the switching-state of a single cell Sk is established by two logical signals (Sk1, Sk2), where "1" and "0" represent the "ON" and "OFF" states of each switch. This leads to four different binary combinations, generating three distinct output voltages: +Vdc, 0, and −Vdc. As the cells are in series connection, the combined output voltage of a single phase "x", in the case of "k" total cells, amounts to

$$v_{xN} = \sum_{y=1}^{k} v_{xy} = \sum_{y=1}^{k} V_{dc}(S_{y1} - S_{y2}),\ x = \{a, b, c\} \quad (2)$$

with V_{dc} as the DC-link voltage and k representing the number of cells for each phase.

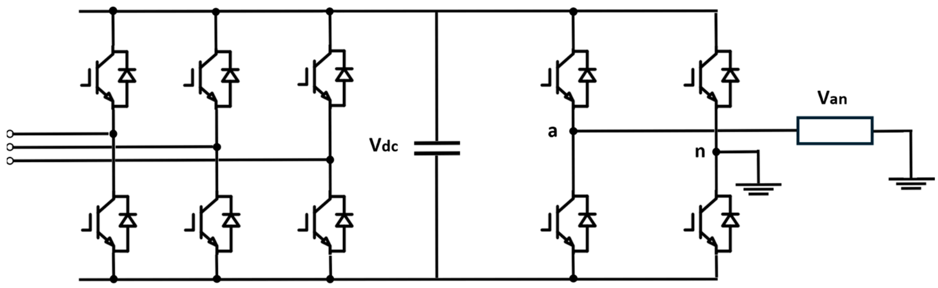

Figure 4. Rectifier and inverter side of CHB cell.

The various output voltage levels can be obtained by substituting all possible configurations of the switching conditions of each cell into Equation (2), thereby deriving the inverter switching table [48].

3.3. Flying Capacitor

The basic structure of a flying capacitor topology is reported in Figure 3 [49–51].

Alternatively, this topology can be represented in a more modular form, commonly referred to as a multicell, as depicted in Figure 5.

Each converter phase leg comprises three commutation cells connected in series [52,53]. $Cx1$ and $Cx2$, representing the rated voltage level of the FCs, are equal to $2/3 \times$ Vdc and $1/3 \times$ Vdc, respectively. In [54], Meynard and Foch developed a technique in order to charge the FCs to the preferred voltage level in the converter initialization process.

Table 2 depicts the switching configurations of a single phase of a 4L-FC-VSC [55–57]. Redundant switch states, exhibiting a different polarity of the FC currents, are employed to balance the voltages across the FCs. Aggregating all three phases, the 4L-FC-VSC encompasses $L^3 = 4^3 = 64$ distinct switching states [58–60].

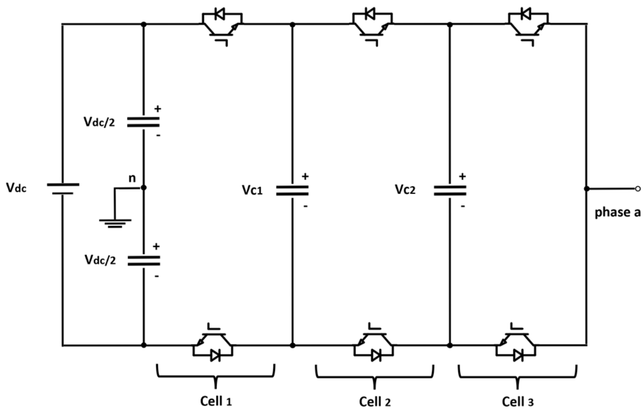

Figure 5. Single phase FC multilevel converter.

Table 2. Single phase 4L-FC-VSC switching table.

Output Voltage VxN	**Gate Signals**			**Capacitor Current**	
	Sx1	**Sx2**	**Sx3**	**Icx1**	**Icx2**
Vdc/2	1	1	1	0	0
Vdc/6	1	1	0	0	+ix
	1	0	1	+ix	−ix
	0	1	1	−ix	0
−Vdc/6	1	0	0	+ix	0
	0	1	0	−ix	+ix
	0	0	1	0	−ix
−Vdc/2	0	0	0	0	0

3.4. Main Modulation Methods

In this section, a brief description of the main modulation techniques employed in MLCs is presented. What differentiates the modulation techniques for MLCs is the switching frequency. Some methods synchronize their switches with the fundamental frequency and are known as low-frequency methods, whereas others operate at much higher frequencies, earning the label of high-frequency methods. The most widely used high-frequency technique is sinusoidal pulse-width modulation (SPWM) [61]. In SPWM, the reference voltage is compared with one or more carrier signals, depending on the number of levels, to generate the desired gate signals. Although SPWM is popular due to its simplicity and robustness, it has limitations, such as voltage self-balancing difficulties and an impossibility to achieve the maximum modulation index without injecting the third harmonic.

Space vector modulation (SVM) is another well-known method that addresses the drawbacks of SPWM. SVM can be easily applied to various multilevel topologies.

The core idea behind SVM is to activate three adjacent vectors relative to a reference vector during a sampling time. The switching times (V_j, V_{j+1}, and V_{j+2}) corresponding to these adjacent vectors can be calculated using an equation based on the volt-second balancing principle.

$$V^* = \frac{(T_j V_j + T_{j+1} V_{j+1} + T_{j+2} V_{j+2})}{T} \tag{3}$$

SVM offers several advantages beyond those mentioned earlier, such as efficient utilization of dc-bus voltage and the possibility to obtain maximum modulation index in a natural way, lower values of the current ripples than SPWM, and ease of implementation using a digital signal processor (DSP).

These advantages position SVM as an excellent choice for high-voltage, high-power applications.

However, as the number of levels increases in multilevel inverters, the number of redundant states also grows. While this flexibility enhances voltage balancing, it simultaneously introduces complexity. For instance, controlling a five-level SVM-based inverter is significantly more intricate than managing a three-level counterpart.

High-frequency techniques like SPWM and SVM result in more commutations per cycle, leading to increased switching losses. Nevertheless, the overall quality of their output is superior.

In contrast, low-frequency switching techniques such as selective harmonic elimination (SHE), space vector control (SVC), and direct torque control (DTC) serve specific applications, each tailored to its unique requirements.

As mentioned, all these modulation techniques can be implemented in all the typical MLC topologies. As regards the CHB, the preferred method is phase-shifted pulse-width modulation (PS-PWM), due to the inherent modularity of the converter [61–63]. In this method, each cell is independently modulated using unipolar PWM with a common reference signal. By introducing a phase shift across all carrier signals within each cell, a stepped multilevel waveform is generated. Notably, the optimal output voltage quality is achieved when employing 180°/k phase shifts between the carriers in a k-cell inverter.

PS-PWM is the best choice also for FCs. Unlike the CHB, where each cell employs three-level outputs, the FC operates with two-level output voltages per cell. Specifically, the FC introduces a 360°/k phase shift among the carriers, where k represents the number of cells [64]. Additionally, bipolar PWM is utilized in the FC, in contrast to unipolar PWM. Other relevant techniques have been proposed, including field-oriented control combined with a phase disposition (PD) carrier-based sine-triangle modulation for the four-level FC-VSC [61]. In this modulation scheme, one-sixth of third harmonics is added to the reference signals. To achieve balanced capacitors in a PD sine-triangle modulation, three 120° phase-shifted trapezoidal carriers are employed within each of the three modulation bands (1 to 1/3, 1/3 to −1/3, and −1/3 to −1).

Regarding NPCs, one of the most relevant issues is the balancing of the neutral point, which has been a topic of great interest for researchers and engineers in recent years.

The most common modulation strategies for NPCs are multiple carrier PWMs, SVM, and SHE, which can be adapted and extended for the multilevel case [65].

3.5. Comparison Summary

In this summarizing paragraph the three classical MLC topologies discussed above are schematically compared in Table 3 regarding efficiency, total harmonic distortion (THD), switch count, power level, applications, and modulation strategies.

As regards THD, its level in MLCs is influenced by several factors, including the number of levels, switching frequency, DC voltage, the modulation technique, and other design parameters. To compare the THD performance of the three classical topologies, some simulation tests have been conducted in a MATLAB/Simulink environment. These simulations have been performed with a switching frequency of 3 kHz and a DC voltage of 400 V, with the resulting output voltage THD levels shown in Figures 6–8.

Table 3. NPC, CHB and FC comparison.

	NPC	CHB	FC
Efficiency	Typically high due to reduced switching losses, especially at lower switching frequencies. However, the efficiency decreases as the number of levels increases due to the additional power losses in the clamping diodes. (96–98%)	High, particularly at higher power levels, because of reduced compo nent stress and the ability to distribute power conversion across multiple modules. (97–99%)	Generally lower compared to the NPC due to the additional power losses associated with charging and discharging the capacitors. Requires careful management of capacitor voltages to maintain efficiency. (94–97%)
THD	Low THD due to the availability of multiple voltage levels that reduce the steps in the output waveform. However, achieving low THD requires precise balancing of capacitor voltages.	Very low THD due to the independent operation of each H-bridge, which can be modulated to produce a near-sinusoidal output waveform. The modularity allows for better harmonic performance.	Generally low THD similar to NPC. The flexibility in voltage levels allows for fine-tuning of the output waveform, thus reducing THD. However, the THD is influenced by the capacitor voltage balancing.
Power Level	Suitable for medium to high-power applications. Typically used in the range of several MW [31].	Highly scalable, making it suitable for a wide range of power levels, from low to very high-power applications, reaching several tens of MW [43].	Generally used in medium-power applications, usually in the range of several hundred kW to a few MW [56].
Switch Count	Moderate, but increases significantly with the number of levels. Requires additional clamping diodes which add to the complexity.	Lower relative to NPC and FC for the same number of levels, since each H-bridge operates independently with fewer components.	High, due to the requirement of multiple capacitors and switches for each level. This increases rapidly as more levels are added.
Applications	Widely used in power transmission systems, HVDC, STATCOMs, and medium-voltage drives [29].	Extensively used in renewable energy applications (solar inverters, wind turbines), FACTS devices, electric vehicles, and medium to high-voltage drives [44].	Suitable for applications requiring high modularity and redundancy, such as high-voltage medical equipment and aerospace systems [54].
Modulation Strategies	Typically employs carrier-based PWM techniques, including phase disposition, phase opposition disposition, and phase-shifted PWM. SVM is also used for higher performance [65].	Phase-shifted PWM or SHE are the most widely used. The modular structure allows for flexible and independent control of each H-bridge module, making it easier to implement advanced modulation strategies [64].	Similar to NPC, it uses carrier-based PWM and SVM. Additionally, balancing the capacitor voltages requires specialized control algorithms [61].

It is important to note that increasing the number of levels significantly reduces the THD. For instance, an 11-level CHB converter can achieve an output voltage THD level lower than 10%. Moreover, it has to be mentioned that referring to the simulation results shown in Figures 6–8, in the case of a 2-level converter, the resulting THD is around 45%.

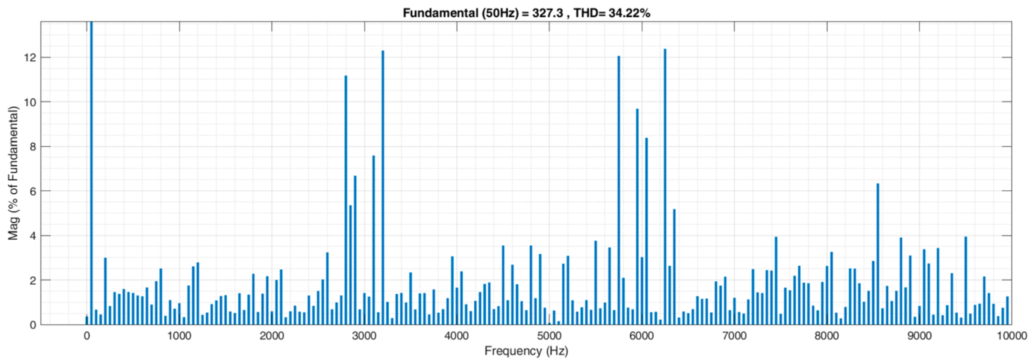

Figure 6. Output voltage THD of a 3-level NPC.

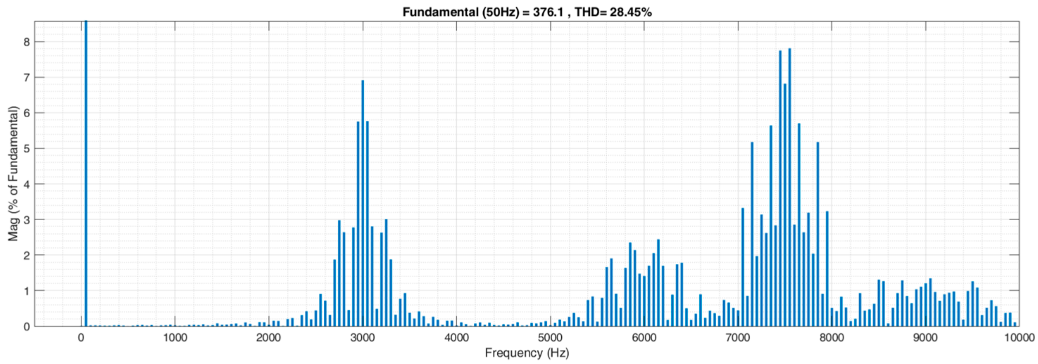

Figure 7. Output voltage THD of a 3-level CHB.

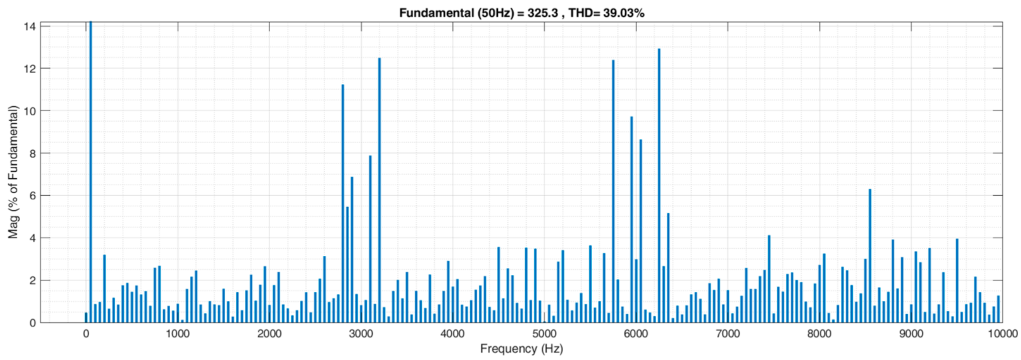

Figure 8. Output voltage THD of a 3-level FC.

4. Recent Advances and New Multilevel Topologies

Figure 9 shows a classification of the most common high-power converter structures in the industry.

Since the inception of the first multilevel topologies nearly five decades ago, numerous variations and novel multilevel converter architectures have been presented in the technical literature. Several of these new configurations consist of modifications in the three classical structures discussed earlier, or combinations thereof. As a matter of fact, for this reason these topologies are called hybrid MLCs. These hybrid configurations combine the features of two of the three classical architectures (NPC, CHB, and FC), in order to obtain the advantages of each, achieve higher voltage levels, and reduce the system complexity. Some of the topologies proposed in the literature in recent years, which gained attention for some high-power applications are the active NPC (ANPC) [66], the T-type converter [67], the various CHB-FC combined architectures proposed in [68,69], or the FC-NPC combined converters introduced in [70,71]. Among the newer topologies that have seen practical adoption, the architectures presented in this study are the modular multilevel converter (MMC), the matrix multilevel converter (M3C), the multiplexed multilevel converter (xPlexed), the five-level H-bridge NPC (5L-HNPC) and the three-level active NPC (ANPC).

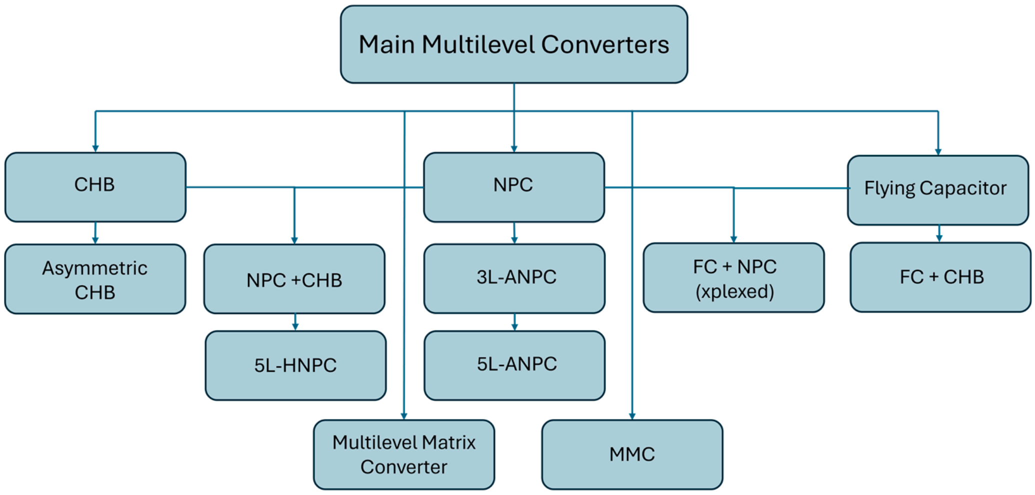

Figure 9. Main multilevel converters in the industry.

4.1. Modular Multilevel Converter

The modular multilevel converter (MMC) was first introduced in the literature by Marquardt [72]. This topology has become one of the most attractive multilevel structures for medium- and high-voltage applications. As a matter of fact, the MMC emerged as a novel solution to address the challenges associated with voltage scalability, reliability, and efficiency in multilevel converters [73–75]. Its distinctive architecture comprises multiple series-connected sub-modules, typically equipped with IGBTs or IGCTs, arranged in a modular fashion. The topology of the MMC enables precise control of the output voltage through adjusting the pulse-width modulation (PWM) of individual sub-modules, allowing for superior voltage quality and reduced harmonic distortion [76–78]. Moreover, the modular design inherently provides fault-tolerance capabilities, as failures in individual sub-modules do not necessarily lead to complete system shutdown.

Since its inception, the MMC has undergone significant developments and optimizations to enhance its performance and applicability across various domains [79–82]. Early research focused on refining control strategies to achieve optimal voltage balancing among sub-modules and maximizing converter efficiency. Subsequent advancements explored extending the MMC's functionality to applications such as high-voltage direct current (HVDC) transmission systems, flexible alternating current transmission systems (FACTS), renewable energy integration, and motor drives [83–86]. Notably, efforts have been directed toward improving the MMC's dynamic response and grid synchronization capabilities, crucial for ensuring stability and reliability in modern power systems.

Structurally, the MMC consists of multiple series-connected HB sub-modules. The voltage across each submodule is independently controlled through a combination of PWM techniques, ensuring precise modulation of the output voltage waveform. The capacitor voltage balancing among sub-modules is achieved through dedicated control algorithms, which actively regulate the charging and discharging of capacitors to maintain voltage symmetry and mitigate circulating currents. Figure 10 shows the topology of the MMC, and the most common sub-module is reported in Figure 11.

Functionally, the MMC operates by synthesizing the desired output voltage waveform from the individual voltage levels of its sub-modules. By adjusting the switching states of the sub-modules based on the desired output voltage reference, the converter generates a staircase-like voltage waveform with reduced harmonic content. This waveform can closely approximate sinusoidal voltage waveforms, thereby improving the quality of the output voltage and minimizing harmonic distortion. Additionally, the MMC's inherent modularity and fault-tolerant design contribute to its robustness and reliability in demanding operating conditions. In summary, the MMC represents a significant advancement in power electronics, offering unparalleled voltage scalability, reliability, and efficiency. Its modular architecture, coupled with advanced control strategies, enables precise voltage control and superior performance across a wide range of applications. As research and development efforts continue to unfold, the MMC remains a focal point of investigation and innovation in the field of multilevel converters, promising continued advancements and widespread adoption in modern power systems.

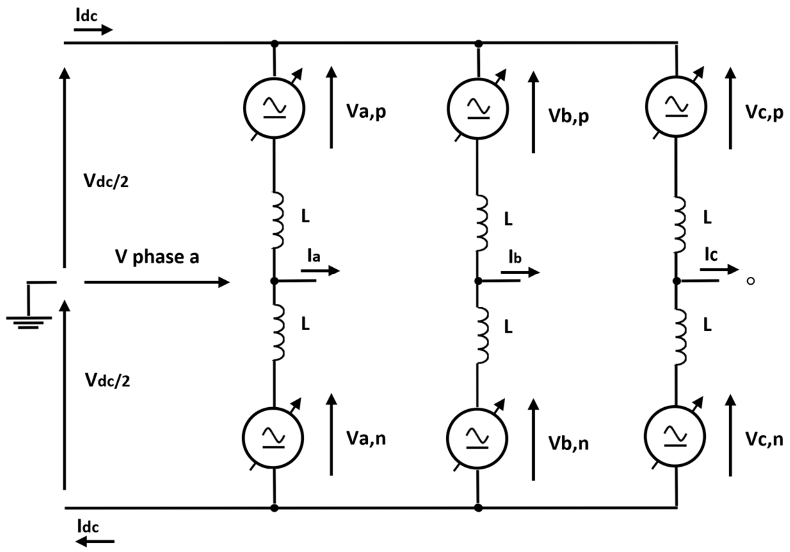

Figure 10. Modular multilevel converter structure.

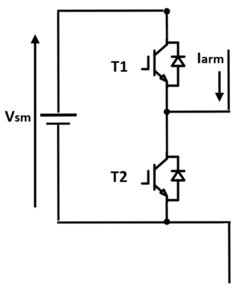

Figure 11. Most common MMC sub-module.

4.2. Matrix Multilevel Converter

Several direct AC/AC MMCs have been proposed over the last years for various applications, including a single-phase-to-single-phase configuration with four arms, a three-phase-to-single-phase setup with six arms, and a three-phase to three-phase configuration with either six or nine arms. Among these, a notable topology is the nine-arm three-phase to three-phase structure, also referred to as the modular multilevel matrix converter (M3C) or triple-star bridge-cells (TSBC). Its circuit configuration resembles a 3-by-3 matrix and has garnered significant attention due to its potential applications in power grid interconnection, low-frequency AC power transmission, and driving low-speed high-torque motors. Compared to other converters, the M3C offers relatively lower power requirements for semiconductors and sub-module capacitors [87–90].

Figure 12 illustrates the primary circuit layout of the M3C, which establishes connectivity between a three-phase load system and a three-phase supply system through nine branches. Notably, the M3C functions as a direct AC/AC converter devoid of a DC-link capacitor, a characteristic typically found in two-stage AC/DC/AC converters. As a result, it enables bidirectional power conversion while simultaneously controlling the sinusoidal current waveform on the input side, regardless of power factors. Unlike the MMC, the M3C experiences minimal capacitor voltage fluctuation during low-frequency operation, rendering it more suitable for high-torque low-speed drive applications, particularly in offshore wind power low-frequency AC transmission systems [91–93].

Initially proposed by Erickson and Al-Naseem without branch inductors [93], the M3C employs a space vector modulation-based control strategy to synthesize the output voltage and maintain balanced capacitor voltages. However, in a M3C where each branch comprises n modules, the complexity arises from the 3^{9n} potential switching states, making implementation challenging. Additionally, as each branch functions as a controlled voltage source, only five branches can switch simultaneously to prevent short circuits.

To address this limitation, a M3C structure with branch inductors was introduced, wherein each branch operates as a controlled current source. This modification enables the utilization of common multilevel carrier modulation strategies, such as phase-shift PWM and phase-disposition PWM, simplifying control mechanisms.

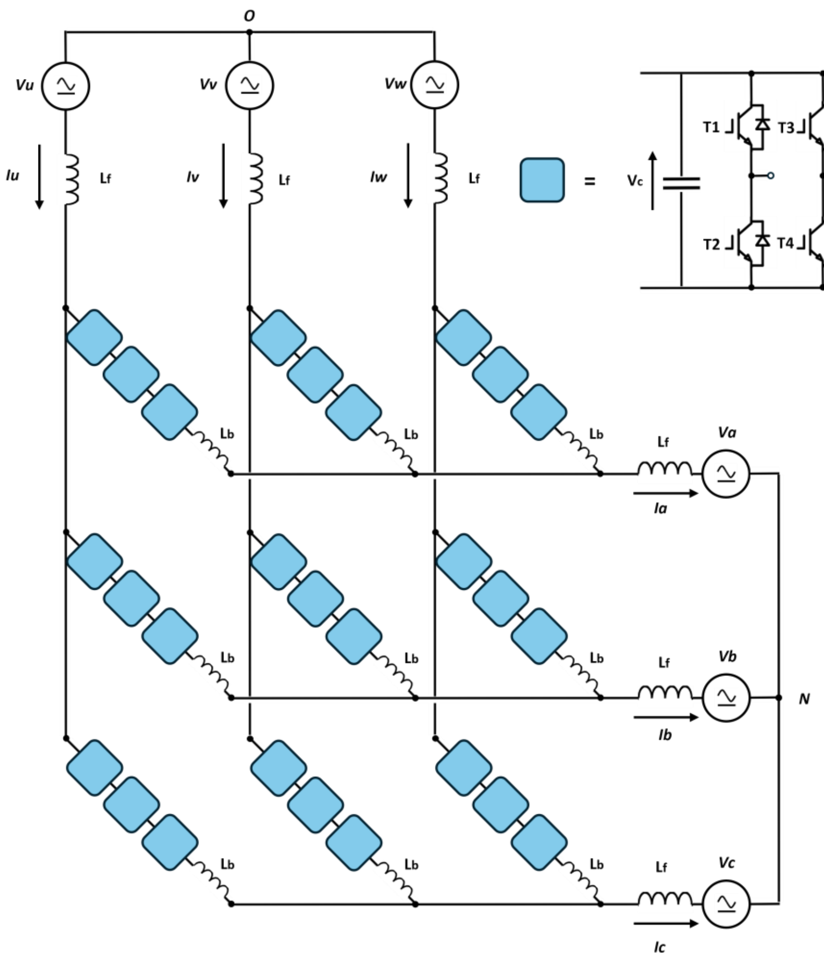

Figure 12. Matrix multilevel converter.

Among the several advantages offered by the M3C topology over traditional converter topologies, one can find the following:

1. Enhanced power quality: by synthesizing multi-level output voltages, the M3C can significantly reduce harmonic distortion and voltage ripple, thereby improving power quality [94,95].
2. High-voltage capability: the modular structure of the M3C enables scalability to higher voltage levels, making it suitable for high-voltage applications such as renewable energy systems, electric vehicle charging, and grid-scale energy storage.

3. Improved efficiency: with advanced control algorithms and modulation techniques, the M3C can achieve high efficiency levels, minimizing losses and improving overall system performance [96].
4. Flexibility and versatility: the M3C topology offers flexibility in terms of voltage levels and modulation strategies, allowing for customization to fulfill specific system requirements.

In recent years, there has been a growing interest in the development of advanced control strategies, modulation techniques, and fault-tolerant schemes for the M3C. Researchers are actively exploring innovative approaches to further improve the performance, reliability, and efficiency of M3C-based systems, paving the way for widespread adoption in various industrial sectors [97–99].

4.3. Multiplexed Converter

The structure of the multiplexed converter topology is depicted in Figure 13 [100]. It comprises 24 switches and integrates two distinct configurations: the FC and the NPC topologies. The initial FC located on the upper side manages the upper dc-bus, while the subsequent FC handles the lower portion of the dc-bus [101]. Consequently, both top and bottom FCs function as dc–dc converters and act as multiplexers. Each FC provides four voltage levels (0, $1/2Vdc$, $1/3Vdc$, and $1/6Vdc$ for the top side and 0, $-1/2Vdc$, $-1/3Vdc$, and $-1/6Vdc$ for the bottom side), resulting in the NPC topology being capable of delivering seven voltage levels (0, $\pm1/2Vdc$, $\pm1/3Vdc$, and $\pm1/6Vdc$) in a single phase.

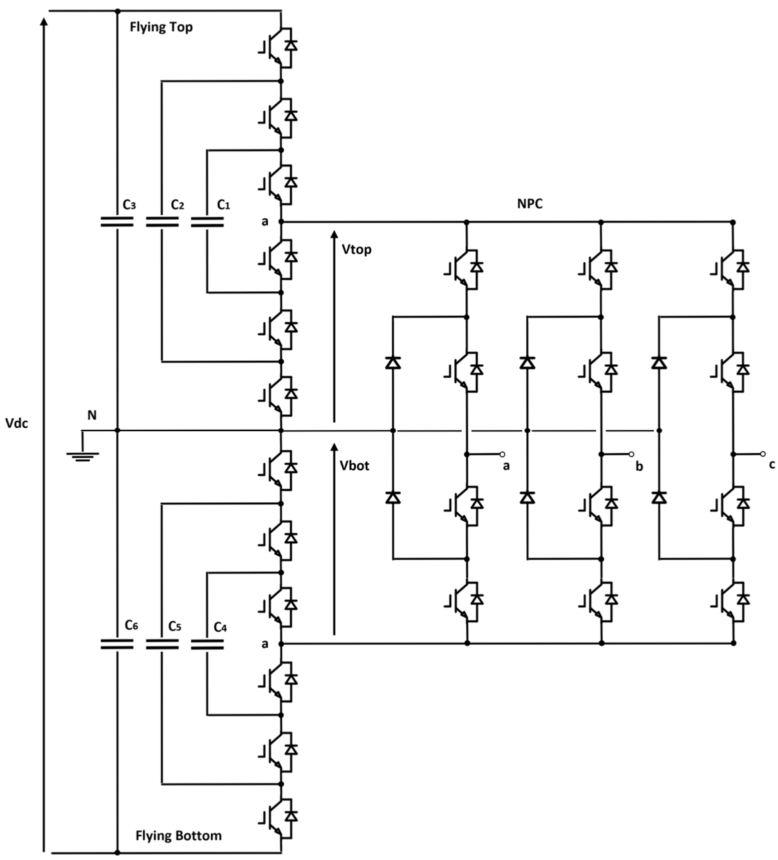

Figure 13. Multiplexed multilevel converter.

The primary advantage of this setup is the elimination of the need for filters, allowing the utilization of cost-effective silicon components or alternatively, SiC devices to enhance efficiency and power density [101–103]. Regarding modulation, pulse-width modulation (PWM) remains the prevalent technique for this topology. Figure 14 [100] illustrates the implemented modulation scheme for the modulation index below and above 0.5.

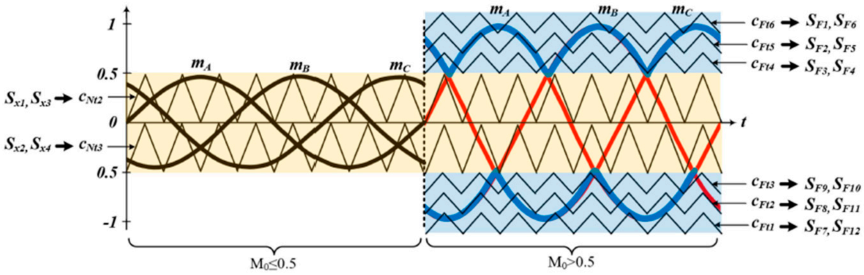

Figure 14. PWM technique for the multiplexed converter.

When M0 $\leq$ 0.5, the top and bottom FCs provide $\pm 1/3Vdc$ (assuming SF3, SF5, SF6, SF7, SF8, and SF10 are actively conducting in the on state), and two carrier signals (cNt2, cNt3) are compared with the modulating signals to derive control signals for the power semiconductors within the NPC.

For M0 > 0.5, it is observed that both the upper and lower segments of the modulation signals (blue line) are regulated by the FCs, while the shifts in the modulation signals (red line) are overseen by the NPC converter. Control signals for the switches within the bottom FC are generated by comparing the lower modulating signal (highlighted in blue) with three carrier signals (c*Ft1*, c*Ft2*, c*Ft3*), while control signals for the switches within the top FC are derived by comparing the greater modulating signal (blue line) with three carrier signals (c*Ft4*, c*Ft5*, c*Ft6*). The results of the comparison between the modulating signals (red) and the two carrier signals (c*Nt2*, c*Nt3*) produce the control signals for the switching devices within the NPC.

The multiplexed converter topology offers an interesting alternative for multilevel converters, potentially reducing the number of high-frequency semiconductors required and thereby lowering the overall cost of the converter. It is well suited for high-power applications, offering various advantages like very high efficiency, optimal voltages, and current waveforms quality, but it can also find space in PV systems, energy storage systems, UPS systems, and MV drives.

4.4. 5L-HNPC

NPC converters are a cornerstone of multilevel converter technology, offering high-quality voltage waveforms with lower harmonic content. To overcome certain limitations of the conventional NPC design such as clamping diode losses and decreased efficiency at higher voltage levels, new variants like H-NPC and A-NPC have been introduced in recent years. These advanced topologies are designed to merge the advantages of NPCs with improved performance characteristics to fulfill the requirements of modern power conversion systems. The H-NPC converter is an evolution of the traditional NPC topology which integrates elements of the CHB topology. This converter topology consists of an H-bridge arrangement of two conventional 3L-NPC phase legs, forming a 5L-HNPC converter as depicted in Figure 15, initially introduced in [104].

Combining the three voltage levels of each leg of the NPC (Vdc/2, 0, −Vdc/2) five distinct output levels can be achieved (Vdc, Vdc/2, 0, −Vdc/2, −Vdc). Comparable to the conventional H-bridge configuration, this setup necessitates an isolated DC source for each H-bridge to prevent DC-link short circuits. Consequently, a transformer with three secondary three-phase windings is necessary to supply the H-bridge of each phase of the converter.

The complexity of the transformer brings along an attractive feature: improved input-side power quality achieved through the phase-shifting transformer and multi-pulse rectifier configuration. This setup effectively cancels low-order harmonics up to the 25th, resulting in a notable reduction in the input current THD and obviating the need for filters, similar to the CHB topology.

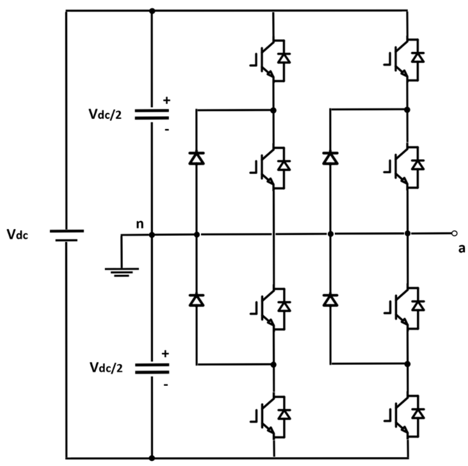

Figure 15. One-phase 5L-HNPC converter.

In practical applications, this converter is typically encountered with a 36-pulse rectifier system, supporting a power range of 2–7 MW (air cooled) or 5–22 MW (water cooled). The H-NPC converter typically employs IGBTs or SiC MOSFETs for switching, with the H-bridge section providing additional voltage levels without the need for clamping diodes, and compensates for the neutral-point potential drift, maintaining voltage balance across the DC-link capacitors. This topology has gained considerable attention in recent years [105,106].

It achieves lower switching losses compared to traditional NPC converters, together with a better management of the neutral-point voltage, reducing the risk of voltage imbalance, and an overall high efficiency, particularly in applications requiring medium-to high-voltage levels. Some drawbacks are the higher cost and the system complexity, requiring sophisticated control algorithms, compared to traditional NPC converters.

H-NPC converters are ideal for medium-voltage motor drives, where efficiency and voltage quality are critical, even if they can also find applications in renewable energy integration systems and in electrical vehicle systems, in particular in fast-charging systems [107–110].

4.5. 3L-ANPC

As mentioned above, the 3L-NPC classical topology presents a challenge due to the unequal distribution of losses between the inner and outer switching devices within each converter leg. This imbalance stems from the separate cooling systems for the semiconductors, resulting in asymmetrical semiconductor-junction temperature distribution. Consequently, this affects the design of the cooling system and imposes limitations on the maximum power rating, output current, and switching frequency of the converter, particularly when using IGCT technology. This issue can be mitigated by using clamping switches instead of the neutral clamping diodes, allowing for an adjustable route for the neutral current, providing regulation of the loss distribution among the switching devices [111]. Unlike clamping diodes, which allow current to freewheel through the upper or lower clamping diode based on current polarity when generating the zero-voltage level, clamping switches enable directing the current through a specific clamping path. This feature facilitates control over power loss distribution, addressing the limitations of the 3L-NPC and enabling significantly higher power rates [66]. These additional components, termed active neutral clamping switches, transform the topology into an active neutral-point-clamped (ANPC) converter [112], as depicted in Figure 16.

This innovative converter topology has sparked significant interest since its introduction, leading to extensive research efforts. It is quickly attracting attention from both academic and industrial sectors [113–115]. By actively controlling the clamping switches, the A-NPC converter can achieve more flexible and efficient switching patterns, reducing the stress on the power devices and the switching losses, leading to higher overall efficiency and improving performance, in particular for high-power applications. In addition, by optimizing the switching sequences, a very low output voltage THD level can be achieved, making it suitable for high-power quality applications. An interesting derivative topology of the 3L-ANPC is the 5L-ANPC, which also gained more attention in recent years [116,117]. As for the H-NPC topology, the increased system complexity can be considered a disadvantage, together with a higher component count, resulting in a higher cost and size of the converter. Regarding the applications, ANPC converters are well suited for high-power industrial drives, grid applications with renewable energies, and HVDC systems [116–118].

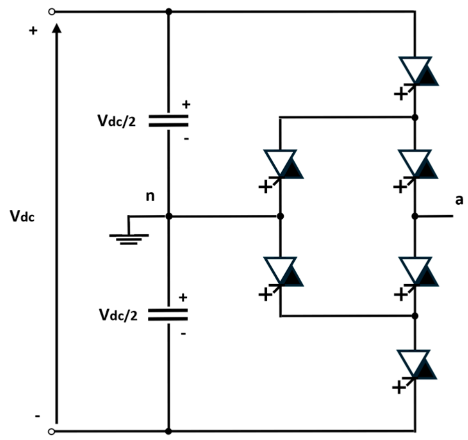

Figure 16. Single phase 3L-ANPC converter.

5. Future Improvements and Perspectives

In this paragraph, some of the future development trends regarding MLCs are presented. The ongoing advancements in semiconductor technology, control strategies, and converter design will continue to expand the capabilities of multilevel converters, making them even more fundamental in the future landscape of power electronics.

The development of advanced control strategies is a crucial aspect for future improvements in the field of MLCs. Sophisticated control algorithms such as model predictive control and adaptive control are essential for managing the increasing complexity of multilevel converters, especially in dynamic and fault-prone environments.

A second fundamental aspect is the integration of wide-bandgap semiconductors: further integration of SiC and GaN devices could significantly increase efficiency and reduce thermal management challenges, particularly in high-power applications.

Another crucial point is the modularity of the converter topology: enhancing the modularity of converters like MMCs and CHBs can reduce maintenance costs and improve fault tolerance, making them more attractive for large-scale industrial applications.

Research into better harmonic filtering techniques and novel modulation strategies could also help reduce THD even further, improving power quality and reducing the need for extensive filtering.

Regarding the applications, as renewable energy sources will continue to proliferate, multilevel converters will increasingly be integrated with energy storage systems, requiring advances in bidirectional power flow and energy management strategies.

As already mentioned in the paper, the electrification of transportation will drive demand for compact, efficient, and high-power converters, particularly in fast-charging infrastructure and onboard power systems.

Lastly, MLCs will also play a crucial role in smart-grid and micro-grid applications where they will be required to handle distributed energy resources, provide auxiliary services, and ensure grid stability.

In order to summarize and give the reader a better understanding of what shown in the previous Section, Tables 4 and 5 have been reported to compare the five MLC topologies.

Table 4. Comparison of the five considered MLCs.

Parameter	MMC	M3C	Multiplexed	5L-H-NPC	3L-A-NPC
Efficiency	97–99% (high) [73–75].	~97% [89].	93–98% [101,102].	96–98% [107].	95–97% [111].
THD	<3% [75].	~3% [88].	~6% [100,101].	<4% [105].	<6% [111].
Power Level	Up to 100 s MW.	Up to 1 MW.	Up to 500 kW [102].	5–20 MW [106].	1–5 MW [66].
Switch Count	12n if half-bridge or 24n if full-bridge (n = sub-modules) [73].	36n (n = sub-modules) [88–90].	30 (7 level) [100].	24 [105].	18 [66,112].
Voltage levels	2n + 1 (n = submodules) [73–75].	2n + 1 (n = sub-modules) [89,90].	7 [100–102].	5 [105,106].	3 [111].

Table 5. Comparison of the five considered MLCs regarding advantages, disadvantages and modulations.

Parameter	MMC	M3C	Multiplexed	5L-H-NPC	3L-A-NPC
Advantages	High robustness and reliability, high scalability for high-voltage applications, high efficiency due to reduced switching frequency [80].	Direct AC–AC conversion without DC link, and reduced harmonic distortion and voltage ripple [89–92].	Reduced switch count compared to other topologies, flexible topology for various applications [102, 103].	High efficiency and reduced switching losses, lower THD compared to traditional 3-level converters [104,108].	Improved efficiency and THD compared to standard 2-level converters, suitable for medium-power applications [66,112,113].
Disadvantages	Complex control and balancing of sub-module capacitors, high component count and size [82–85].	Complex control and commutation schemes, higher THD in output voltage compared to MMC [90–92].	Limited voltage scalability, higher THD than MMC and H-NPC [103].	Complex circuit design and additional components, requires complex control strategies [109].	Limited to medium voltage levels, higher component count than 2-level converters [114–117].
Modulation Strategies	PS-PWM, Nearest Level-PWM, SHE [4,79].	SVM [4].	PWM [4,100].	SVM, SHE, PD-PWM [4].	SVM [4].

6. Conclusions

More than five decades have passed since the first introduction in the technical literature and in the market of the multilevel converters. During these years, it has become evident that multilevel converters offer significant advantages over traditional two-level converters in terms of improved efficiency, reduced harmonic distortion, and enhanced voltage and current waveforms, and their relevance in the industry is nowadays well known, especially in high-power applications. In summary, this paper has provided an overview and discussion about the topological properties and interrelationships of the main multilevel converter structures. The evolution of multilevel converter technology has witnessed remarkable advancements in recent years, driven by the increasing demand for high-power, high-efficiency conversion systems in various industrial applications such as renewable energy integration, electric vehicles, and grid-connected systems. The development of new semiconductor devices, along with innovative control algorithms and modulation schemes, has further expanded the capabilities and performance of multilevel converters.

Despite the considerable progress made, several challenges and opportunities remain for future research and development in the field of multilevel converters. These include the optimization of converter topologies for specific applications, the enhancement of converter efficiency and reliability, the integration of advanced control and modulation techniques, and the exploration of new semiconductor materials and device technologies. In addition, thermal management continues to be a critical issue, especially in high-power applications. Research is ongoing to address these challenges, with a focus on advanced control strategies and the integration of intelligent fault-detection mechanisms.

Author Contributions: Conceptualization, M.M. and L.V.; Formal analysis, A.F., M.P. and S.C.; Investigation, A.B., S.C., A.F. and L.V.; Simulations, S.C.; Methodology, A.B., S.C., A.F. and M.P.;

Supervision, M.M. and L.V.; Writing—original draft, S.C.; Writing—review and editing, M.M., A.F. and L.V. All authors have read and agreed to the published version of the manuscript.

Funding: This research received no external funding.

Conflicts of Interest: The authors declare no conflicts of interest.

References

1. Qashqai, P.; Sheikholeslami, A.; Vahedi, H.; Al-Haddad, K. A Review on Multilevel Converter Topologies for Electric Transportation Applications. In Proceedings of the 2015 IEEE Vehicle Power and Propulsion Conference (VPPC), Montreal, QC, Canada, 19–22 October 2015; pp. 1–6.
2. Gonzatti, R.B.; Li, Y.; Amirabadi, M.; Lehman, B.; Peng, F.Z. An Overview of Converter Topologies and Their Derivations and Interrelationships. *IEEE J. Emerg. Sel. Top. Power Electron.* **2022**, *10*, 6417–6429. [CrossRef]
3. Ebrahimi, J.; Babaei, E.; Gharehpetian, G.B. A New Multilevel Converter Topology with Reduced Number of Power Electronic Components. *IEEE Trans. Ind. Electron.* **2012**, *59*, 655–667. [CrossRef]
4. Edpuganti, A.; Rathore, A.K. A Survey of Low Switching Frequency Modulation Techniques for Medium-Voltage Multilevel Converters. *IEEE Trans. Ind. Appl.* **2015**, *51*, 4212–4228. [CrossRef]
5. Fang, J.; Blaabjerg, F.; Liu, S.; Goetz, S. A Review of Multilevel Converters with Parallel Connectivity. *IEEE Trans. Power Electron.* **2021**, *36*, 12468–12489. [CrossRef]
6. Gupta, K.K.; Ranjan, A.; Bhatnagar, P.; Sahu, L.K.; Jain, S. Multilevel Inverter Topologies with Reduced Device Count: A Review. *IEEE Trans. Power Electron.* **2016**, *31*, 135–151. [CrossRef]
7. Harbi, I.; Rodriguez, J.; Poorfakhraei, A.; Vahedi, H.; Guse, M.; Trabelsi, M.; Abdelrahem, M.; Ahmed, M.; Fahad, M.; Lin, C.H. Common DC-Link Multilevel Converters: Topologies, Control and Industrial Applications. *IEEE Open J. Power Electron.* **2023**, *4*, 512–538. [CrossRef]
8. Kouro, S.; Malinowski, M.; Gopakumar, K.; Pou, J.; Franquelo, L.G.; Wu, B.; Rodriguez, J.; A Pérez, M.; I Leon, J. Recent Advances and Industrial Applications of Multilevel Converters. *IEEE Trans. Ind. Electron.* **2010**, *57*, 2553–2580. [CrossRef]
9. Marchesoni, M.; Mazzucchelli, M. Multilevel converters for high power AC drives: A review. In Proceedings of the IEEE International Symposium on Industrial Electronics (ISIE'93), Budapest, Hungary, 1–3 June 1993; pp. 38–43.
10. Vijeh, M.; Rezanejad, M.; Samadaei, E.; Bertilsson, K. A General Review of Multilevel Inverters Based on Main Submodules: Structural Point of View. *IEEE Trans. Power Electron.* **2019**, *34*, 9479–9502. [CrossRef]
11. Wu, M.; Li, Y.W.; Konstantinou, G. A Comprehensive Review of Capacitor Voltage Balancing Strategies for Multilevel Converters Under Selective Harmonic Elimination PWM. *IEEE Trans. Power Electron.* **2021**, *36*, 2748–2767. [CrossRef]
12. Yuan, X. Ultimate Generalized Multilevel Converter Topology. *IEEE Trans. Power Electron.* **2021**, *36*, 8634–8639. [CrossRef]
13. Nami, A.; Liang, J.; Dijkhuizen, F.; Demetriades, G.D. Modular Multilevel Converters for HVDC Applications: Review on Converter Cells and Functionalities. *IEEE Trans. Power Electron.* **2015**, *30*, 18–36. [CrossRef]
14. Rauf, A.M.; Abdel-Monem, M.; Geury, T.; Hegazy, O. A Review on Multilevel Converters for Efficient Integration of Battery Systems in Stationary Applications. *Energies* **2023**, *16*, 4133. [CrossRef]
15. Bughneda, A.; Salem, M.; Richelli, A.; Ishak, D.; Alatai, S. Review of Multilevel Inverters for PV Energy System Applications. *Energies* **2021**, *14*, 1585. [CrossRef]
16. Aouichak, I.; Jacques, S.; Bissey, S.; Reymond, C.; Besson, T.; Le Bunetel, J.-C. A Bidirectional Grid-Connected DC–AC Converter for Autonomous and Intelligent Electricity Storage in the Residential Sector. *Energies* **2022**, *15*, 1194. [CrossRef]
17. Harlisca, C.; Szabo, L.; Frosini, L.; Albini, A. Bearing faults detection in induction machines based on statistical processing of the stray fluxes measurements. In Proceedings of the 2013 9th IEEE International Symposium on Diagnostics for Electric Machines, Power Electronics and Drives-(SDEMPED 2013), Valencia, Spain, 27–30 August 2013; pp. 371–376.
18. Li, L.; Xu, G.; Sha, D.; Liu, Y.; Sun, Y.; Su, M. Review of Dual-Active-Bridge Converters with Topological Modifications. *IEEE Trans. Power Electron.* **2023**, *38*, 9046–9076. [CrossRef]
19. Sun, P.; Tian, Y.; Pou, J.; Konstantinou, G. Beyond the MMC: Extended Modular Multilevel Converter Topologies and Applications. *IEEE Open J. Power Electron.* **2022**, *3*, 317–333. [CrossRef]
20. Maragliano, G.; Marchesoni, M.; Parodi, G.; Vaccaro, L. A new generalized fault tolerant space vector modulator for cascaded multilevel converters. In Proceedings of the IECON 2011 37th Annual Conference of IEEE Industrial Electronics, Melbourne, Australia, 7–10 November 2011; pp. 1069–1074.
21. Maragliano, G.; Marchesoni, M.; Vaccaro, L. A new N-level space vector modulator for cascaded multilevel converters. In Proceedings of the 2013 15th European Conference on Power Electronics and Applications (EPE), Lille, France, 3–5 September 2013.
22. Gregor, R.; Toledo, S.; Maqueda, E.; Pacher, J. Part I—Advancements in Power Converter Technologies: A Focus on SiC-MOSFET-Based Voltage Source Converters. *Energies* **2013**, *16*, 5994. [CrossRef]
23. McMurray, W. Fast Response Stepped-Wave Switching Power Converter Circuit. U.S. Patent 3581212, 25 May 1971.
24. Dickerson, J.A.; Ottaway, G.H. Transformerless Power Supply with Line to Load Isolation. U.S. Patent 3596369, 3 August 1971.
25. Baker, R.H. High-Voltage Converter Circuit. U.S. Patent 4203151, 13 May 1980.

26. Nabae, A.; Takahashi, I.; Akagi, H. A New Neutral-Point-Clamped PWM Inverter. *IEEE Trans. Ind. Appl.* **1981**, *IA-17*, 518–523. [CrossRef]
27. Marchesoni, M.; Mazzucchelli, M.; Tenconi, S. A non conventional power converter for plasma stabilization. In Proceedings of the PESC '88 Record 19th Annual IEEE Power Electronics Specialists Conference, Kyoto, Japan, 11–14 April 1990; pp. 122–129.
28. Meynard, T.; Foch, H. Dispositif Électronique de Conversion D'énergie Électrique. French Patent 2679715B1, 29 January 1993.
29. Song, W.; Saeed, M.S.R.; Yu, B.; Li, J.; Guo, Y. Model Predictive Current Control with Reduced Complexity for Five-Phase Three-Level NPC Voltage-Source Inverters. *IEEE Trans. Transp. Electrif.* **2022**, *8*, 1906–1917. [CrossRef]
30. Sanchez-Ruiz, A.; Mazuela, M.; Fernandez-Rebolleda, H.; Ceballos, S.; Perez-Basante, A.; Ibanez-Hidalgo, I.; Zubiaga, M.; Pou, J.; Beniwal, N.; Konstantinou, G. DC-Link Neutral Point Control for 3L-NPC Converters Utilizing Selective Harmonic Elimination–PWM. *IEEE Trans. Ind. Electron.* **2022**, *69*, 8633–8644. [CrossRef]
31. Marchesoni, M.; Vaccaro, L. Extending the operating range in Diode-Clamped Multilevel inverters with Active Front Ends. In Proceedings of the 2012 IEEE International Energy Conference (ENERGYCON 2012), Florence, Italy, 9–12 September 2012.
32. Vazquez, S.; Acuna, P.; Aguilera, R.P.; Pou, J.; Leon, J.I.; Franquelo, L.G. DC-Link Voltage-Balancing Strategy Based on Optimal Switching Sequence Model Predictive Control for Single-Phase H-NPC Converters. *IEEE Trans. Ind. Electron.* **2020**, *67*, 7410–7420. [CrossRef]
33. Wang, K.; Zheng, Z.; Xu, L.; Li, Y. Neutral-Point Voltage Balancing Method for Five-Level NPC Inverters Based on Carrier-Overlapped PWM. *IEEE Trans. Power Electron.* **2021**, *36*, 1428–1440. [CrossRef]
34. Zhang, L.; Zheng, Z.; Li, C.; Ju, P.; Wu, F.; Gu, Y.; Chen, G. A Si/SiC Hybrid Five-Level Active NPC Inverter with Improved Modulation Scheme. *IEEE Trans. Power Electron.* **2020**, *35*, 4835–4846. [CrossRef]
35. Khan, A.A.; Khan, U.A.; Ahmed, F.; Cha, H.; Ahmed, S.A. Improved NPC Inverters without Short-Circuit and Dead-time Issues. *IEEE Trans. Power Electron.* **2021**, *37*, 2180–2190. [CrossRef]
36. Dong, Z.; Wang, C.; Cui, K.; Cheng, Q.; Wang, J. Neutral-Point Voltage-Balancing Strategies of NPC-Inverter Fed Dual Three-Phase AC Motors. *IEEE Trans. Power Electron.* **2021**, *36*, 3181–3191. [CrossRef]
37. Fedele, E.; Iannuzzi, D.; Tricoli, P.; Del Pizzo, A. NPC-Based Multi-Source Inverters for Multimode DC Rail Traction Systems. *IEEE Trans. Transp. Electrification* **2023**, *9*, 1289–1299. [CrossRef]
38. Casini, D.; Marchesoni, M.; Puglisi, L. Sliding mode multilevel control for improved performances in power conditioning systems. *IEEE Trans. Power Electron.* **1995**, *10*, 453–463. [CrossRef]
39. Wu, X.; Xiong, C.; Yang, S.; Yang, H.; Feng, X. A Simplified Space Vector Pulsewidth Modulation Scheme for Three-Phase Cascaded H-Bridge Inverters. *IEEE Trans. Power Electron.* **2020**, *35*, 4192–4204. [CrossRef]
40. Chai, M.; Gorla, N.B.Y.; Panda, S.K. Fault Detection and Localization for Cascaded H-Bridge Multilevel Converter with Model Predictive Control. *IEEE Trans. Power Electron.* **2020**, *35*, 10109–10120. [CrossRef]
41. Lewicki, A.; Odeh, I.C.; Morawiec, M. Space Vector Pulsewidth Modulation Strategy for Multilevel Cascaded H-Bridge Inverter With DC-Link Voltage Balancing Ability. *IEEE Trans. Ind. Electron.* **2023**, *70*, 1161–1170. [CrossRef]
42. Liu, C.; Gao, N.; Cai, X.; Li, R. Differentiation Power Control of Modules in Second-Life Battery Energy Storage System Based on Cascaded H-Bridge Converter. *IEEE Trans. Power Electron.* **2020**, *35*, 6609–6624. [CrossRef]
43. Lashab, A.; Sera, D.; Kerekes, T.; Terriche, Y.; Bouzid, A.; Vasquez, J.C.; Guerrero, J.M. A Cascaded H-Bridge with Integrated Boosting Circuit. *IEEE Trans. Power Electron.* **2021**, *36*, 18–22. [CrossRef]
44. Liu, P.; Duan, S. Derivation of the Generalized Phase-Shifted Angles by Using Phasor Diagrams for the CHB Converter with Unbalanced DC Voltage Sources. *IEEE Trans. Ind. Electron.* **2021**, *68*, 12002–12009. [CrossRef]
45. Ma, J.; Wang, X.; Blaabjerg, F.; Song, W.; Wang, S.; Liu, T. Multisampling Method for Single-Phase Grid-Connected Cascaded H-Bridge Inverters. *IEEE Trans. Ind. Electron.* **2020**, *67*, 8322–8334. [CrossRef]
46. Marquez, A.; Monopoli, V.G.; Tcai, A.; Leon, J.I.; Buticchi, G.; Vazquez, S.; Liserre, M.; Franquelo, L.G. Discontinuous-PWM Method for Multilevel N-Cell Cascaded H-Bridge Converters. *IEEE Trans. Ind. Electron.* **2021**, *68*, 7996–8005. [CrossRef]
47. Nasiri, M.R.; Farhangi, S.; Rodriguez, J. Model Predictive Control of a Multilevel CHB STATCOM in Wind Farm Application Using Diophantine Equations. *IEEE Trans. Ind. Electron.* **2019**, *66*, 1213–1223. [CrossRef]
48. Neyshabouri, Y.; Monfared, K.K.; Iman-Eini, H.; Farhadi-Kangarlu, M. Symmetric Cascaded H-Bridge Multilevel Inverter with Enhanced Multi-Phase Fault Tolerant Capability. *IEEE Trans. Ind. Electron.* **2022**, *69*, 8739–8750. [CrossRef]
49. Ghias, A.M.Y.M.; Pou, J.; Capella, G.J.; Acuna, P.; Agelidis, V.G. On Improving Phase-Shifted PWM for Flying Capacitor Multilevel Converters. *IEEE Trans. Power Electron.* **2016**, *31*, 5384–5388. [CrossRef]
50. Ghias, A.M.Y.M.; Pou, J.; Capella, G.J.; Agelidis, V.G.; Aguilera, R.P.; Meynard, T. Single-Carrier Phase-Disposition PWM Implementation for Multilevel Flying Capacitor Converters. *IEEE Trans. Power Electron.* **2015**, *30*, 5376–5380. [CrossRef]
51. Kampitsis, G.; Batzelis, E.I.; Mitcheson, P.D.; Pal, B.C. A Clamping-Circuit-Based Voltage Measurement System for High-Frequency Flying Capacitor Multilevel Inverters. *IEEE Trans. Power Electron.* **2022**, *37*, 12301–12315. [CrossRef]
52. Lin, X.; Burgos, R.; Dong, D. Improved Variable Switching Frequency Control for Capacitor Voltage Ripple Regulation in Multilevel Flying Capacitor Converter. *IEEE Trans. Power Electron.* **2023**, *38*, 5700–5705. [CrossRef]
53. Liu, J.; Dong, D. A Flying Capacitor Hybrid Modular Multilevel Converter with Reduced Number of Submodules and Power Losses. *IEEE Trans. Ind. Electron.* **2023**, *70*, 3293–3302. [CrossRef]
54. Meynard, T.; Foch, H.; Thomas, P.; Courault, J.; Jakob, R.; Nahrstaedt, M. Multicell converters: Basic concepts and industry applications. *IEEE Trans. Ind. Electron.* **2002**, *49*, 955–964. [CrossRef]

55. Du, S.; Wu, B.; Zargari, N.R. A Startup Method for Flying-Capacitor Modular Multilevel Converter (FC-MMC) with Effective Damping of LC Oscillations. *IEEE Trans. Power Electron.* **2017**, *32*, 5827–5834. [CrossRef]
56. Du, S.; Wu, B.; Zargari, N.R. Current Stress Reduction for Flying-Capacitor Modular Multilevel Converter. *IEEE Trans. Power Electron.* **2019**, *34*, 184–191. [CrossRef]
57. Du, S.; Wu, B.; Zargari, N.R.; Cheng, Z. A Flying-Capacitor Modular Multilevel Converter for Medium-Voltage Motor Drive. *IEEE Trans. Power Electron.* **2017**, *32*, 2081–2089. [CrossRef]
58. Ebrahimi, J.; Karshenas, H.; Eren, S.; Bakhshai, A. A Fast-Decoupled Space Vector Modulation Scheme for Flying Capacitor-Based Multilevel Converters. *IEEE Trans. Power Electron.* **2021**, *36*, 14539–14549. [CrossRef]
59. Ebrahimi, J.; Shahnooshi, S.; Eren, S.; Karshenas, H.; Bakhshai, A. Optimized Switching Frequency Voltage Balancing Schemes for Flying Capacitor Based Multilevel Converters. *IEEE Trans. Ind. Electron.* **2023**, *70*, 10775–10788. [CrossRef]
60. Farivar, G.; Ghias, A.M.Y.M.; Hredzak, B.; Pou, J.; Agelidis, V.G. Capacitor Voltages Measurement and Balancing in Flying Capacitor Multilevel Converters Utilizing a Single Voltage Sensor. *IEEE Trans. Power Electron.* **2017**, *32*, 8115–8123. [CrossRef]
61. Carrara, G.; Gardella, S.; Marchesoni, M.; Salutari, R.; Sciutto, G. A new multilevel PWM method: A theoretical analysis. *IEEE Trans. Power Electron.* **1992**, *7*, 497–505. [CrossRef]
62. Gemma, F.; Tresca, G.; Formentini, A.; Zanchetta, P. Balanced Charging Algorithm for CHB in an EV Powertrain. *Energies* **2023**, *16*, 5565. [CrossRef]
63. Comparatore, L.; Ayala, M.; Kali, Y.; Rodas, J.; Pacher, J.; Renault, A.; Gregor, R. Discrete-Time Sliding Mode Current Control for a Seven-Level Cascade H-Bridge Converter. *Energies* **2023**, *16*, 2481. [CrossRef]
64. Mersche, S.C.; Schwendemann, R.; Hiller, M. Validation of the Quasi-Two-Level Operation for a Flying Capacitor Converter in Medium-Voltage Applications. *Energies* **2023**, *16*, 2797. [CrossRef]
65. Barros, J.D.; Rocha, L.; Silva, J.F. Backstepping Control of NPC Multilevel Converter Interfacing AC and DC Microgrids. *Energies* **2023**, *16*, 5515. [CrossRef]
66. Bruckner, T.; Bernet, S.; Guldner, H. The Active NPC Converter and Its Loss-Balancing Control. *IEEE Trans. Ind. Electron.* **2005**, *52*, 855–868. [CrossRef]
67. Dwivedi, D.; Singh, S.; Kaushik, S.; Semail, E.; Nguyen, N.K.; Chinmaya, K.A. T-Type Multilevel Inverters: A Comparative Performance Analysis. In Proceedings of the 2023 IEEE 3rd International Conference on Sustainable Energy and Future Electric Transportation (SEFET), Bhubaneswar, India, 9–12 August 2023; pp. 1–6.
68. Babaei, E.; Gowgani, S.S. Hybrid Multilevel Inverter Using Switched Capacitor Units. *IEEE Trans. Ind. Electron.* **2014**, *61*, 4614–4621. [CrossRef]
69. Dargahi, V.; Sadigh, A.K.; Khorasani, R.R.; Rodriguez, J. Active Voltage Balancing Control of a Seven-Level Hybrid Multilevel Converter Topology. *IEEE Trans. Ind. Electron.* **2022**, *69*, 74–89. [CrossRef]
70. Abdelghani, A.B.-B.; Abdelghani, H.B.; Richardeau, F.; Blaquière, J.-M.; Mosser, F.; Slama-Belkhodja, I. Versatile Three-Level FC-NPC Converter with High Fault-Tolerance Capabilities: Switch Fault Detection and Isolation and Safe Postfault Operation. *IEEE Trans. Ind. Electron.* **2017**, *64*, 6453–6464. [CrossRef]
71. Chatterjee, S.; Kastha, D. A Five-Level Six-Switch Hybrid FC-NPC based Unidirectional Power Converter Topology with Enhanced Reactive Power Capability. *IEEE J. Emerg. Sel. Top. Power Electron.* **2024**, *12*, 4400–4412. [CrossRef]
72. Lesnicar, A.; Marquardt, R. An innovative modular multilevel converter topology suitable for a wide power range. In Proceedings of the IEEE Bologna Power Tech Conference Proceedings, Bologna, Italy, 23–26 June 2003; Volume 3, p. 6. [CrossRef]
73. Cano, T.C.; Rodriguez, A.; Castro, I.; Lamar, D.G. Distributed Input Multiport MMC Based Power Converter for AC and DC Loads. *IEEE Trans. Power Electron.* **2023**, *38*, 7971–7975. [CrossRef]
74. Fan, X.; Qiu, D.; Zhang, B.; Chen, Y.; Xie, F.; Yuan, C. Recognition and Analysis of Unexpected Modes of Modular Multilevel Converter. *IEEE Access* **2021**, *9*, 90195–90202. [CrossRef]
75. Farnesi, S.; Marchesoni, M.; Vaccaro, L. Reliability improvement of Modular Multilevel Converter in HVDC systems. In Proceedings of the 2016 Power Systems Computation Conference (PSCC), Genova, Italy, 22–24 June 2016.
76. Gao, X.; Tian, W.; Yang, Q.; Chai, N.; Rodriguez, J.; Kennel, R.; Heldwein, M.L. Model Predictive Control of a Modular Multilevel Converter Considering Control Input Constraints. *IEEE Trans. Power Electron.* **2024**, *39*, 636–648. [CrossRef]
77. Gray, P.A.; Lehn, P.W.; Yakop, N. A Modular Multilevel DC–DC Converter with Flying Capacitor Converter Like Properties. *IEEE Trans. Ind. Electron.* **2022**, *69*, 6774–6783. [CrossRef]
78. Guo, G.; Song, Q.; Zhao, B.; Rao, H.; Xu, S.; Zhu, Z.; Liu, W. Series-Connected-Based Offshore Wind Farms with Full-Bridge Modular Multilevel Converter as Grid- and Generator-side Converters. *IEEE Trans. Ind. Electron.* **2020**, *67*, 2798–2809. [CrossRef]
79. Maragliano, G.; Marchesoni, M.; Vaccaro, L. Optimal operation mode for Modular Multilevel Converter based HVDC. In Proceedings of the 2014 International Symposium on Power Electronics, Electrical Drives, Automation and Motion (SPEEDAM 2014), Ischia, Italy, 18–20 June 2014.
80. Marchesoni, M.; Vaccaro, L. Study of the MMC circulating current for optimal operation mode in HVDC applications. In Proceedings of the 2015 17th European Conference on Power Electronics and Applications (EPE'15 ECCE-Europe), Geneva, Switzerland, 8–10 September 2015.
81. Patro, S.K.; Shukla, A. Modular Directed Series Multilevel Converter for HVDC Applications. *IEEE Trans. Ind. Appl.* **2020**, *56*, 1618–1630. [CrossRef]

82. Qin, F.; Gao, F.; Tang, Y.; Xu, T.; Wang, J.; Niu, D.C. Configuration and Operation of Nine-Arm Modular Multilevel Converter with Improved Hybrid Submodules. *IEEE Trans. Power Electron.* **2021**, *36*, 6389–6403. [CrossRef]
83. Reddy, G.A.; Shukla, A. Circulating Current Optimization Control of MMC. *IEEE Trans. Ind. Electron.* **2021**, *68*, 2798–2811. [CrossRef]
84. Wang, C.; Xu, J.; Pan, X.; Gong, W.; Zhu, Z.; Xu, S. Impedance Modeling and Analysis of Series-Connected Modular Multilevel Converter (MMC) and its Comparative Study with Conventional MMC for HVDC Applications. *IEEE Trans. Power Deliv.* **2022**, *37*, 3270–3281. [CrossRef]
85. Xu, Y.; Zhang, Z.; Wang, G.; Xu, Z. Modular Multilevel Converter with Embedded Energy Storage for Bidirectional Fault Isolation. *IEEE Trans. Power Deliv.* **2021**, *37*, 105–115. [CrossRef]
86. Yin, T.; Xu, C.; Lin, L.; Jing, K. A SiC MOSFET and Si IGBT Hybrid Modular Multilevel Converter with Specialized Modulation Scheme. *IEEE Trans. Power Electron.* **2020**, *35*, 12623–12628. [CrossRef]
87. Yao, W.; Liu, J.; Lu, Z. Distributed Control for the Modular Multilevel Matrix Converter. *IEEE Trans. Power Electron.* **2019**, *34*, 3775–3788. [CrossRef]
88. Wang, C.; Zheng, Z.; Wang, K.; Yang, B.; Zhou, P.; Li, Y.G. Analysis and Control of Modular Multilevel Matrix Converters under Branch Fault Conditions. *IEEE Trans. Power Electron.* **2021**, *37*, 1682–1699. [CrossRef]
89. Luo, J.; Zhang, X.-P.; Xue, Y.; Gu, K.; Wu, F. Harmonic Analysis of Modular Multilevel Matrix Converter for Fractional Frequency Transmission System. *IEEE Trans. Power Deliv.* **2020**, *35*, 1209–1219. [CrossRef]
90. Yu, Z.; Zhang, Z.; Xu, Z. Electromechanical Transient Modeling of the Low-Frequency AC System with Modular Multilevel Matrix Converter Stations. *IEEE Trans. Power Syst.* **2024**, *39*, 921–933. [CrossRef]
91. Urrutia, M.; Cardenas, R.; Clare, J.C.; Diaz, M.; Watson, A. Continuous Set Model Predictive Control for Energy Management of Modular Multilevel Matrix Converters. *IEEE Trans. Power Electron.* **2022**, *37*, 5731–5748. [CrossRef]
92. Liu, S.; Zhao, B.; Wang, G.; Wang, X. An Improved Phasor Method for Modelling and Analysis of Modular Multilevel Matrix Converter. *IEEE Trans. Power Deliv.* **2021**, *36*, 1744–1755. [CrossRef]
93. Erickson, R.W.; Al-Naseem, O.A. A new family of matrix converters. In Proceedings of the IECON'01 27th Annual Conference of the IEEE Industrial Electronics Society (Cat. No.37243), Denver, CO, USA, 29 November–2 December 2001; Volume 2, pp. 1515–1520.
94. Liu, J.; Yue, S.; Yao, W.; Li, W.; Lu, Z. DC Voltage Ripple Optimization of a Single-Stage Solid-State Transformer Based on the Modular Multilevel Matrix Converter. *IEEE Trans. Power Electron.* **2020**, *35*, 12801–12815. [CrossRef]
95. Kienast, J.; Hoffmann, A.; Höer, M.; Bernet, S. Novel Distributed Control Platform and Algorithm for a Modular Multilevel Matrix Converter. *IEEE Trans. Power Electron.* **2023**, *38*, 8089–8101. [CrossRef]
96. Fan, B.; Wang, K.; Zheng, Z.; Xu, L.; Li, Y. Optimized Branch Current Control of Modular Multilevel Matrix Converters Under Branch Fault Conditions. *IEEE Trans. Power Electron.* **2018**, *33*, 4578–4583. [CrossRef]
97. Diaz, M.; Cardenas, R.; Espinoza, M.; Rojas, F.; Mora, A.; Clare, J.C.; Wheeler, P. Control of Wind Energy Conversion Systems Based on the Modular Multilevel Matrix Converter. *IEEE Trans. Ind. Electron.* **2017**, *64*, 8799–8810. [CrossRef]
98. Diaz, M.; Cardenas, R.; Espinoza, M.; Hackl, C.M.; Rojas, F.; Clare, J.C.; Wheeler, P. Vector Control of a Modular Multilevel Matrix Converter Operating Over the Full Output-Frequency Range. *IEEE Trans. Ind. Electron.* **2019**, *66*, 5102–5114. [CrossRef]
99. Bontemps, P.; Milovanovic, S.; Dujic, D. Performance Analysis of Energy Balancing Methods for Matrix Modular Multilevel Converters. *IEEE Trans. Power Electron.* **2023**, *38*, 2910–2924. [CrossRef]
100. Lidozzi, A.; di Benedetto, M.; Meynard, T.A.; Solero, L. Medium-Voltage Seven-Level Multiplexed Converter for AC Applications. *IEEE Open J. Power Electron.* **2023**, *4*, 81–90. [CrossRef]
101. Burguete, E.; Lopez, J.; Zubimendi, I.; Larrazabal, I.; Meynard, T.; Gateau, G. Multilevel voltage source conversion approach: Multiplexed choppers. *IET Power Electron.* **2016**, *9*, 2329–2336. [CrossRef]
102. Kremer, V.; Lacarnoy, A.; Meynard, T.A. New Multi-Level Multiplexed Power Converter Topology for Medium-Voltage Power Drives. In Proceedings of the PCIM Europe Digital Days 2021, International Exhibition and Conference for Power Electronics, Intelligent Motion, Renewable Energy and Energy Management, Online, 3–7 May 2021; pp. 1–8.
103. Odriozola, K.; Meynard, T.A.; Lacarnoy, A. Multi-Level Multiplexed Power Converter Topology for 1500V Applications. In Proceedings of the IECON 2019 45th Annual Conference of the IEEE Industrial Electronics Society, Lisbon, Portugal, 14–17 October 2019; pp. 4405–4410.
104. Carpaneto, M.; Marchesoni, M.; Vaccaro, L. A New Cascaded Multilevel Converter Based on NPC Cells. In Proceedings of the 2007 IEEE International Symposium on Industrial Electronics, Vigo, Spain, 4–7 June 2007.
105. Chen, J.; Zhong, Y.; Wang, C.; Fu, Y. Four-Level Hybrid Neutral Point Clamped Converters. *IEEE J. Emerg. Sel. Top. Power Electron.* **2021**, *9*, 4786–4801. [CrossRef]
106. Etxeberria-Otadui, I.; Lopez-de-Heredia, A.; San-Sebastian, J.; Gaztanaga, H.; Viscarret, U.; Caballero, M. Analysis of a H-NPC topology for an AC traction front-end converter. In Proceedings of the 2008 13th International Power Electronics and Motion Control Conference, Poznan, Poland, 1–3 September 2008; pp. 1555–1561.
107. Tu, H.; Feng, H.; Srdic, S.; Lukic, S. Extreme Fast Charging of Electric Vehicles: A Technology Overview. *IEEE Trans. Transp. Electrif.* **2019**, *5*, 861–878. [CrossRef]
108. Belkhode, S.; Shukla, A.; Doolla, S. Five-Level Hybrid Active-NPC H-Bridge Converter with Novel Space-Vector-Modulation Scheme. *IEEE J. Emerg. Sel. Top. Power Electron.* **2022**, *10*, 4146–4159. [CrossRef]

109. Chamarthi, P.K.; Muduli, U.R.; El Moursi, M.S.; Al-Durra, A.; Al-Sumaiti, A.S.; Al Hosani, K. Improved PWM Approach for Cascaded Five-Level NPC H-Bridge Configurations in Multilevel Inverter. *IEEE Trans. Ind. Appl.* **2024**, *60*, 7048–7060. [CrossRef]
110. Gutierrez, E.; Kouro, S.; Rojas, C.A.; Aguirre, M. Predictive control of an H-NPC converter for single-phase rooftop photovoltaic systems. In Proceedings of the 2015 IEEE Energy Conversion Congress and Exposition, Montreal, QC, Canada, 2–24 September 2015; pp. 3295–3302.
111. Floricau, D.; Floricau, E.; Dumitrescu, M. Natural doubling of the apparent switching frequency using three-level ANPC converter. In Proceedings of the 2008 International School on Nonsinusoidal Currents and Compensation (ISNCC), Łagów, Poland, 10–13 June 2008; pp. 1–6.
112. Brückner, T.; Bernet, S. nLoss balancing in three-level voltage source inverters applying active NPC switches. In Proceedings of the 2001 IEEE 32nd Annual Power Electronics Specialists Conference, Vancouver, BC, Canada, 17–21 June 2001; pp. 1135–1140.
113. Lee, S.-J.; Hyun, S.-W.; Hong, S.-J.; Lee, H.-J.; Won, C.-Y. Predictive thermal modeling for loss distribution method of 3-level active NPC inverter. In Proceedings of the 2015 IEEE International Telecommunications Energy Conference (INTELEC), Osaka, Japan, 18–22 October 2015; pp. 1–5.
114. Lee, B.-G.; Hyun, S.-W.; Lee, H.-J.; Shin, S.-C.; Won, C.-Y.; Lee, T.-G. Convenient thermal modeling for loss distribution of 3-level Active NPC using newton's law. In Proceedings of the 2014 IEEE International Conference on Industrial Technology (ICIT), Busan, Republic of Korea, 26 February-1 March 2014; pp. 409–413.
115. Zhang, B.; Ge, Q.; Tan, L.; Wang, X.; Yu, Y.; Liu, J. A New PWM scheme for loss balancing and neutral-point voltage balancing in three-level active NPC converter. In Proceedings of the 2015 IEEE 10th Conference on Industrial Electronics and Applications (ICIEA), Auckland, New Zealand, 15–17 June 2015; pp. 1128–1133.
116. Wang, K.; Li, Y.; Zheng, Z. A neutral-point potential balancing algorithm for five-level ANPC converters. In Proceedings of the 2011 International Conference on Electrical Machines and Systems (ICEMS), Beijing, China, 20–23 August 2011; pp. 1–5.
117. Sathik, M.J.; Tang, Z.; Yang, Y.; Vijayakumar, K.; Blaabjerg, F. A New 5-Level ANPC Switched Capacitor Inverter Topology for Photovoltaic Applications. In Proceedings of the IECON 2019 45th Annual Conference of the IEEE Industrial Electronics Society, Lisbon, Portugal, 14–17 October 2019; pp. 3487–3492.
118. Belkhode, S.; Shukla, A.; Doolla, S. A Multi-Segment PWM Scheme for Enhanced Hybrid Active NPC H-Bridge Converter. In Proceedings of the 2024 IEEE Applied Power Electronics Conference and Exposition (APEC), Long Beach, CA, USA, 25–29 February 2024; pp. 2712–2717.